Deformation Evaluation of Embedded Antennas in Vehicular Components

E. Sulic, B. Pell, S. John, R. Gupta, W. Rowe K. Ghorbani and K. Zhang

***Abstract*—In this paper, an attempt is made to extend the deformation model of an antenna embedded in vehicular component, where the component consists of a viscoelastic thermoset composite polymer commonly known as Sheet Moulding Compound (SMC). The initial model developed takes into account time dependent heat transfer from the tool surface into the SMC charge and the consequent time dependent viscosity propagation during the initial stage of tool closing and subsequent filling. The required model parameters for viscosity and elasticity have been determined from rheological testing. The extended model examines the effects of some process parameters such as tool closing speed, tool temperature and initial charge temperature. The effect of these parameters on the deformation of the antenna is discussed and compared to experimental findings. In addition the signal quality due to antenna deformation is investigated by comparing simulation and experimental results.**

***Index Terms*: Antenna, Automobile, Car, Communication device, Embedding, Vehicle.**

I. Nomenclature

C_p	specific heat capacity
Ea	activation energy
g	gravity
G	complex viscosity
G'	storage modulus
G''	loss modulus
K	thermal conductivity
λ	relaxation time of the material
m	adjustable variable (rate of change of shear rate)
η	viscosity
η'	complex viscosity component
p	pressure
ρ	density
R	universal gas constant
$\|S_{11}\|$	input port voltage reflection coefficient
T	temperature in Celsius
Tk	reference temperature in Kelvin
t_i	time material is in contact with bottom tool surface
t_j	time material is in contact with bottom tool surface
v	velocity
$\dot{\gamma}$	shear rate

Manuscript received March 18, 2010. This work was supported in part by the Australian Research Council and Composites Materials Engineering under Grant LP0561868.

E. Sulic & S. John are with RMIT University, School of Aerospace, Mechanical & Manufacturing Engineering, Bundoora, VIC 3083 Australia. Corresponding author – S John: Phone +61 3 9925 6007; fax +61 3 9925 6003; e-mail: sabu.john@rmit.edu.au.

B. Pell, W. Rowe & K. Ghorbani are with RMIT University, School of Computer and Electrical Engineering, City Campus, Melbourne, VIC 3001 Australia.

R. Gupta is with RMIT University, School of Civil and Chemical Engineering, City Campus, Melbourne, VIC 3001 Australia.

K. Zhang is with RMIT University, School of Mathematical and Geospatial Sciences, City Campus, Melbourne, VIC 3001 Australia.

II. Introduction

One of the fastest growing uses of SMC material is in the area of manufacturing of vehicle body components for both structural and non-structural applications according to Sarah *et al*. [1]. This trend is accelerating and is driven by Original Equipment Manufacturers (OEM's) and their need for lighter more fuel efficient vehicles. In addition, the use of composite materials such as SMC allows vehicle designers to use more complex component shapes that are not feasible with traditional materials such as stamped steel and aluminium. In the last twenty years the number of entertainment and communication systems in the vehicles has also been expanding. Current services such as GPS, digital radio, and cellular phone, and future services such as collision avoidance radar, vehicle-to-vehicle and vehicle-to-roadside communications require use of antennas to send/receive signals that are necessary for these services to function. Progress in antenna design and their placement in vehicles have manifested itself in traditional 'mast' type antennas being replaced by other type of antennas placed between laminated sheets of glass Lindenmeier *et al.* [2] patch antennas mounted on the inner side of the automotive rear glass Economou *et al*. [3]. Other techniques include variations of 'shark-fin', 'bee-sting' or blade designs used by BMW, Mercedes, Jaguar, Lexus, VW, Opel and Audi, Welbeoff *et al*. [4] and conformal planar designs used by Volvo XC90, Low *et al.* [5] and Gschwendtner *et al.* [6].

The development of one single wideband antenna of which an example can be seen in Figure 1 that is capable of receiving all of the services listed above would represent significant advantage for any OEM. Taking this approach one step further and embedding such an antenna in a composite vehicle body panel, be it the roof, hood or boot, thereby creating a 'smart composite component' would combine benefits of reduced coefficient of drag, lower vehicle weight, reduced assembly complexity and shorter assembly time. These benefits would manifest themselves in

ISBN: 978-988-18210-8-9
ISSN: 2078-0958 (Print); ISSN: 2078-0966 (Online)

form of lower overall design and manufacturing vehicle cost for the OEMs and lower fuel consumption for customers.

During initial embedding trials of such an antenna into SMC, a noticeable antenna deformation was observed, requiring the development of a numerical model capable of predicting this deformation. The numerical model developed is used to investigate change in parameters such as mould temperature, initial material/charge temperature and mould closing speed in order to minimise antenna deformation during the embedding process.

The early work carried out in this field involved understanding the material model for SMC flow based on the experimentally observed kinematics. This included work by Barone *et al.* [7]-[9] in the late 70's and mid 80's, followed by further work by Osswald *et al.* [10]. SMC material kinematics research undertaken by Castro *et al.* [11], [12] and Tucker *et al.* [13] in the late 80's and mid 90's has significantly extended previous work done by Barone. They explored the early models and developed approximate methods to characterise the SMC material based on experimentally measured parameters.

III. MODELING APPROACH

The entire compression moulding cycle consists of five main steps. They are: 1-loading material, 2-tool close, 3-cure material, 4-tool open and 5-unload material. In the model presented, the focus was on only the first two main steps -loading the material and closing of the tool as this is where all of the antenna deformation occurs as seen in Fig 1.

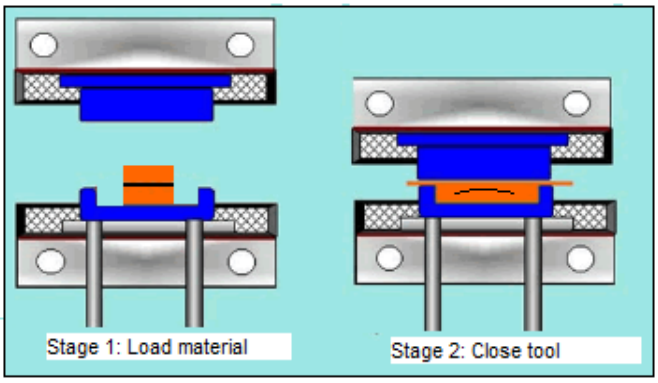

Figure 1: First two stages of compression molding process.

This process can be represented schematically using Maxwell model, as seen in Fig 2.

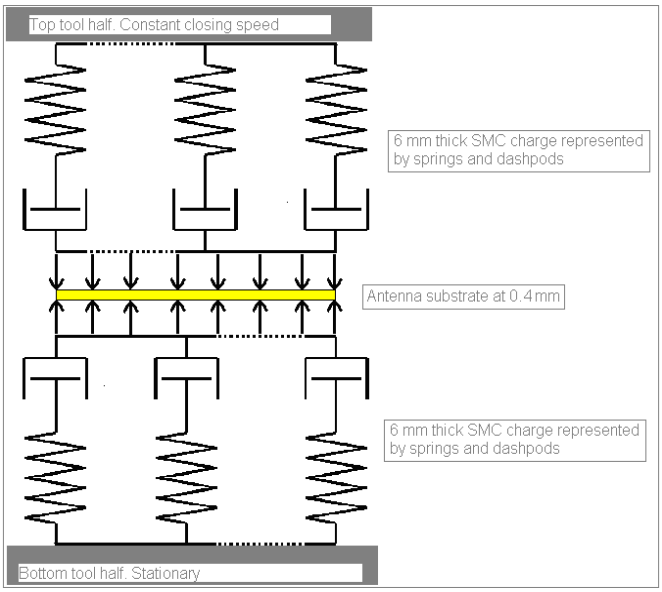

Figure 2: Maxwell model representation of the SMC and the antenna substrate.

The calculation of the net deformation in the antenna using a rheological model requires the use of a scheme which would incorporate the combined effect of temperature, time and viscosity.

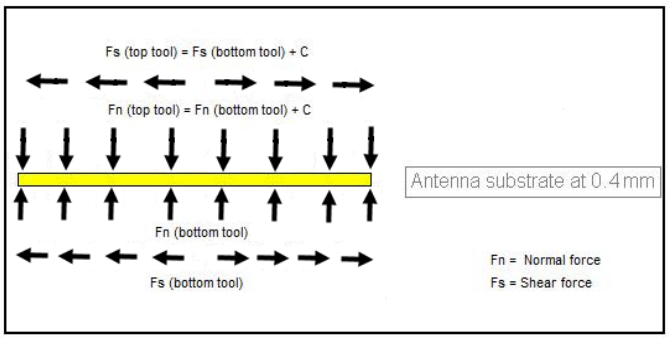

Figure 3: Representation of shear and normal force acting on the antenna.

The following simulation or modeling scheme in Fig 4 was developed in order to meet these needs:

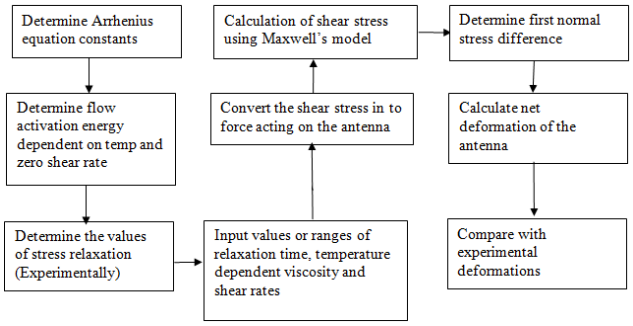

Figure 4: Model flow diagram

IV DEFORMATION CALCULATION

SMC is considered (as is other thermosets) to be an incompressible viscous material which flows inside the tool cavity according to the Navier-Stokes equation, Bird *et al.* [14]:

ISBN: 978-988-18210-8-9
ISSN: 2078-0958 (Print); ISSN: 2078-0966 (Online)

$$\rho\frac{\partial v}{\partial t}-\nabla.\sigma=\rho g \qquad (1)$$
$$\frac{\partial \rho}{\partial t}+\rho\nabla.v=0$$

The viscosity of the material depends on the strain rate, the temperature and the degree of cure. In this case, the degree of cure can be removed from the equation as only the first two steps of the process (comprising the first 10-16 seconds) are considered here:

$$\eta=\eta'(\dot{\gamma})\,f(T)g \qquad (2)$$

The influence of temperature is governed by the Arrhenius law:

$$\eta=\eta_0 e^{-Ea/RT} \qquad (3)$$

Dynamic frequency tests were conducted at three different temperatures (120^0C, 140^0C and 160^0C). The above temperatures were selected as they cover the range of commonly used temperatures in the manufacturing of SMC. The relaxation time and modulus is a function of the Dynamic rheological parameters (G', G" and complex viscosity). The relaxation modulus in terms of the storage modulus (as per Maxwell's model) is given by:

$$\sum G'=\sum\frac{\lambda^2\omega^2}{1+\lambda^2\omega^2} \qquad (4)$$

$$\sum G''=\sum\frac{\lambda\omega}{1+\lambda^2\omega^2} \qquad (5)$$

$$G=G'+iG'' \qquad (6)$$

Fig 5 shows the relaxation times vs frequency obtained for the type of SMC used in this case.

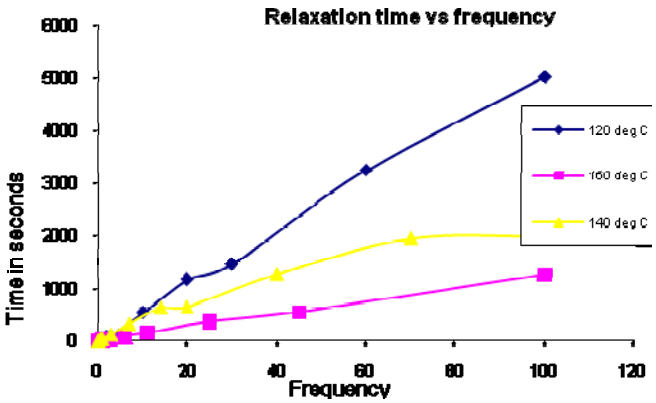

Figure 5 Relaxation time curves for 120^0C, 140^0C and 160^0C, frequency in rad/s and time in seconds.

Heat transfer equation is used to determine time dependant temperature propagation as follows:

$$\rho\overline{Cp}\left(\frac{\partial T}{\partial t}+Vx\frac{\partial T}{\partial x}+Vy\frac{\partial T}{\partial y}+Vz\frac{\partial T}{\partial z}\right)=k\left(\frac{\partial^2 T}{\partial x^2}+\frac{\partial^2 T}{\partial y^2}+\frac{\partial^2 T}{\partial z^2}\right)+\mu\phi_v \qquad (7)$$

This equation is a generalized version of the energy equation. In this case, the temperature profile developed is only due to conduction and hence, it is a static system with no convective heat transport. Therefore Vx=Vy=Vz = 0. Also, for the moment the internal heat generation term is neglected. The curing of the SMC material results in liberation of heat. Hence, to determine the internal heat generation it is important to know the rate constant / degree of curing. Once the rate constant is known then the internal heat generation can also be considered. Significant work has already been done by Fundrinier *et al.* [15] to determine the rate constant for the curing process within the SMC. In this case, the curing process is not very important while determining the temperature profile since the entire process of antenna deformation is complete in the time it takes the top tool to fully close. The time required for closing is a function of the speed of the top tool hence the time of closing varies within the range of 12-16 seconds. Once the antenna is deformed, the generation of internal heat has no effect on any further deformation.

Hence, simplifying the above equation:

$$\rho\overline{Cp}\left(\frac{\partial T}{\partial t}\right)=k\left(\frac{\partial^2 T}{\partial z^2}\right) \qquad (8)$$

Where $k/\rho C_p$ is the biot number. This number is dimensionless.

The values of k, C_p & ρ have been taken from the literature and are:

k = 0.92 W/K-1 (thermal conductivity)
C_p = 1040 J/K-1 (specific heat capacity)
ρ = 1890 kg/m^3 (material density)

The variation in temperature in x and y direction is neglected since the time dependent propagation through the thickness of the material (z direction) is the most important parameter to be considered in this case. Fig 6 shows the variation in viscosity with temperature.

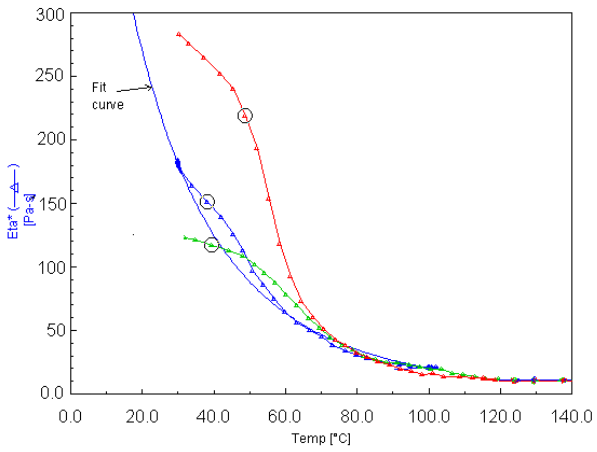

Figure 6: Viscosity vs Temperature.

ISBN: 978-988-18210-8-9
ISSN: 2078-0958 (Print); ISSN: 2078-0966 (Online)

V. SHEAR STRESS CALCULATION

The next step is the calculation of the shear stress acting on the SMC charge. The Maxwell model in conjunction with the relaxation modulus, the shear rate regime and the shear viscosity range can be used to determine the shear stress distribution which can be further used to calculate the net force and the deformation in the antenna. The antenna is embedded in the centre of the SMC charge.

At time t=0, the charge is placed in the tool. The lower surface of the charge is then lying on the bottom face of the heated tool, and hence this lower surface of the charge begins heating by conduction. The top tool however has a time lag of around 10 seconds before the tool closes and it contacts the charge. This time lag results in a transient temperature profile within the SMC charge. The shear stress acting on the antenna is due to the temperature dependent viscosity and the differential stress between the top and the bottom portion of the charge (below and above the antenna). This stress difference results in deformation of the antenna.

Using the Newton's law for viscosity, where shear stress depends on the material viscosity and shear rate:

$$\tau_{12} = \eta_0 \dot{\gamma}_{12} \tag{9}$$

to obtain final equation we get:

$$\tau_{12} = \sum_{t=1}^{i} \frac{\eta}{\lambda^2} \dot{\gamma}_{12} \exp\left(\frac{-t_i}{\lambda}\right) - \frac{\eta.m}{\lambda^3} \exp\left(\frac{-t_i}{\lambda}\right) + c$$

$$\sum_{j=1}^{j} \frac{\eta}{\lambda^2} \dot{\gamma}_{12} \exp\left(\frac{-t_j}{\lambda}\right) - \frac{\eta.m}{\lambda^3} \exp\left(\frac{-t_j}{\lambda}\right) + c \tag{10}$$

VI. FIRST NORMAL STRESS DIFFERENCE

The first normal stress difference $(\tau_{11} - \tau_{22})$ is generated within the material when the material begins to relax after application of a stress. In terms of the spring dashpot model the first normal stress difference is given by:

$$(\tau_{11} - \tau_{22}) = \lambda.(\gamma_{12})^n \tag{11}$$

VII. RESULTS

Table 1 below, shows the summary of the results. It compares the calculated data verses experimental data. Different process parameters have been investigated and their impact on antenna deformation is summarized. The approach taken was to evaluate a range of initial charge temperatures with the standard tool closing speed and tool temperature, then select the temperature with the lowest resultant deformation and evaluate it while changing the tool closing speed. Repeating the same procedure again we have selected initial charge and tool closing speed with lowest resultant antenna deformation and evaluated it against tool temperature.

VIII. METHOD OF INVESTIGATION

Both simulations and measurements were used to investigate the effect of curvature on the antenna performance. The curvature was investigated in four steps of increasing angles: 0°, 22°, 45°, and 90° as per Fig 7.

Table 1: Summary of the results

Run	Charge Temperature	Closing speed of the tool in mm/s	Tool temperature	Calculated deformation in mm	Experimental deformation in mm	Comments
1	30 ˚C	3	150 ˚C	0.58	0.60	Good surface finish and material flow.
2	40 ˚C	3	150 ˚C	0.28	0.32	Good surface finish and material flow.
3	50 ˚C	3	150 ˚C	0.17	0.22	Good surface finish and material flow.
4	60 ˚C	3	150 ˚C	0.12	0.17	Surface finish improved.
5	60 ˚C	2	150 ˚C	0.12	0.17	Improvement in material flow, almost perfect circular flow observed.
6	60 ˚C	4	150 ˚C	0.11	0.15	Good surface finish and material flow.
7	60 ˚C	6	150 ˚C	0.10	0.20	Due to high tool speed poor surface finish and uneven material flow observed.
8	60 ˚C	4	140 ˚C	0.21	0.24	Poor material flow.
9	60 ˚C	4	160 ˚C	0.10	0.13	Improvement in material flow, almost perfect circular flow observed.
10	60 ˚C	4	170 ˚C	0.09	NA	Material starts to crosslink resulting in unacceptable sample finish.

ISBN: 978-988-18210-8-9
ISSN: 2078-0958 (Print); ISSN: 2078-0966 (Online)

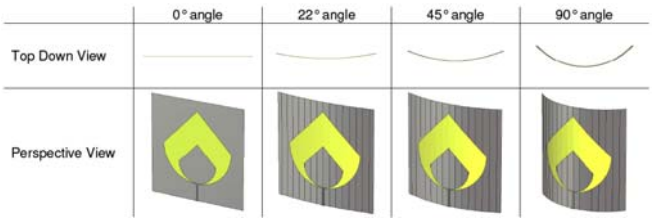

Figure 7 Induced Strain from Curvatures Investigated

Figs 8 to Fig 13 represent impedance matching and radiation pattern results obtained from the simulation software and experimental measurements. These results show good correlation between simulated and measured results. This would indicate that the simulation can be reliably used to obtain signal quality data for future prototype components before physical measurements need to be done as part of the final validation test.

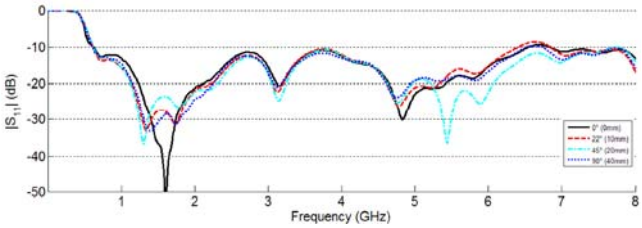

Figure 8 Simulated Impendence Matching Results

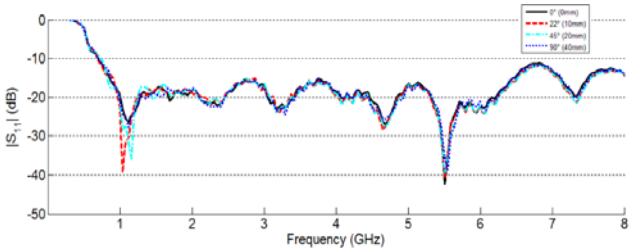

Figure 11 Measured Impendence Matching Results

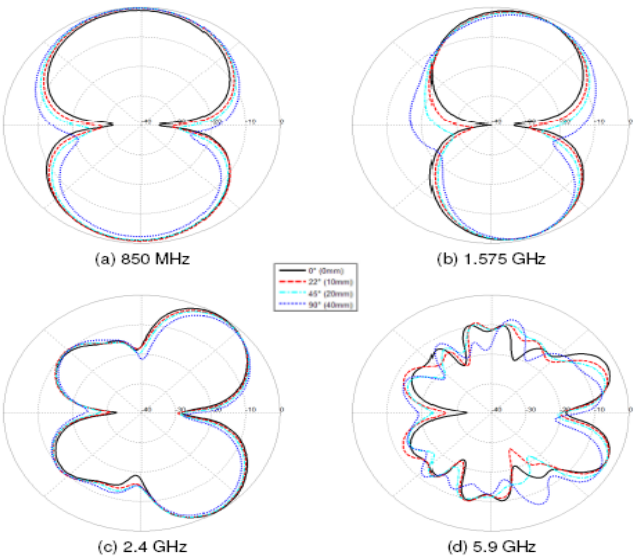

Figure 9 E plane co-polar Simulations

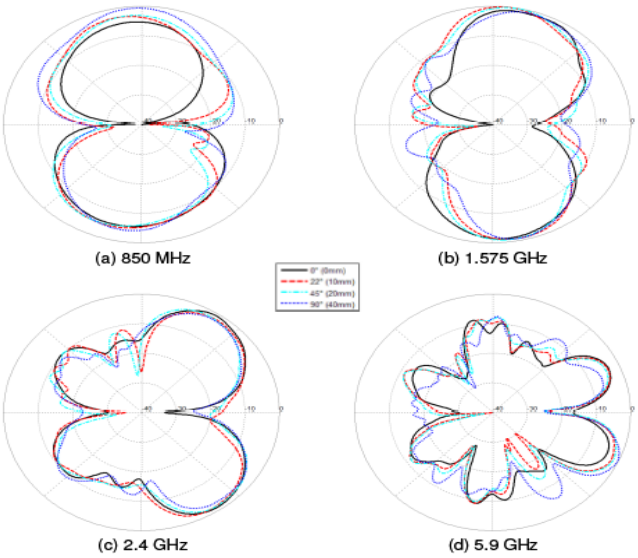

Figure 12 E plane co-polar Measurements

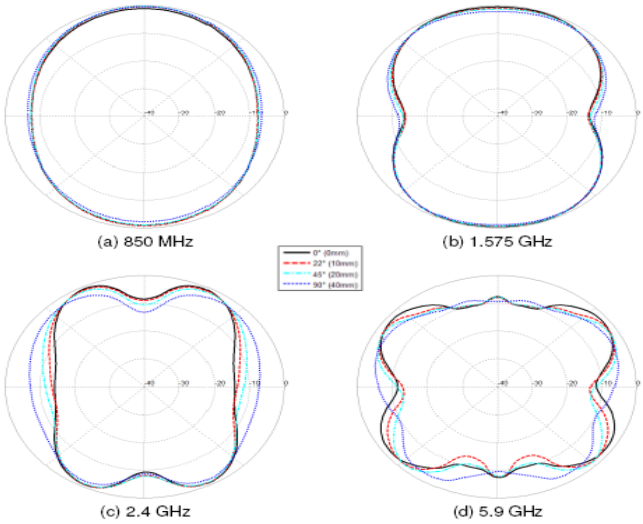

Figure 10 H plane co-polar Simulations

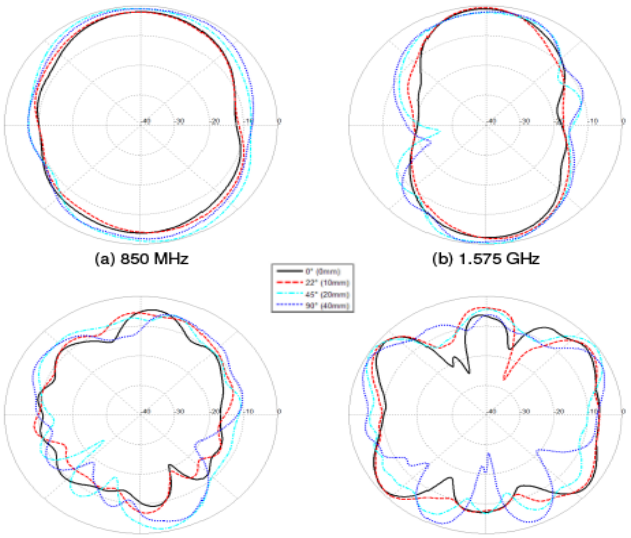

Figure 13 H plane co-polar Measurements

ISBN: 978-988-18210-8-9
ISSN: 2078-0958 (Print); ISSN: 2078-0966 (Online)

IX. DISCUSSION

As seen from the Table 1, the greatest effect on the antenna deformation is observed when the material charge is preheated to 60 ˚C (as in run 4). The impact of other process variables such as tool closing speed and tool temperature generates some additional reduction in antenna deformation. However, this additional benefit is very small. Furthermore, if the tool closing speed is too high it can result in unwanted effects such as poor surface finish and material flow, such as for runs 7 and 10.

Again from Table 1, it can be seen that the correlation between calculated values for antenna deformation and experimentally obtained values for antenna deformation is better for the standard values of tool closing speed and tool temperature, in runs 1 to 4. Once the tool closing speed is increased to 6 mm/sec, as in run 7, or the tool temperature is increased to 170 ˚C, as in run 10, correlation between calculated and experimental values reduces. This is possibly due to the fact that while the material charge is heated up to 60˚C and then subsequently placed in the tool at 170 ˚C, some of the molecules start to crosslink very rapidly resulting in uneven material flow. Behavior of this uneven material flow is more difficult to predict using the material model developed as it does not take into account the degree of material cure in equation 2 and its effects on material viscosity on which the shear stress ultimately depends.

The results for the antenna presented here appear to be resistant to changes in impedance and radiation when curved. Simulations and measurements both reveal only minor shifts in |S11|, with no mismatches occurring. Examination of the radiation results reveals that curvature of the antenna may lead to redirection of radiated energy, creating a shift in the location of the main lobes. Only slight changes to the maximum gain on the order of a few dB, were observed as a result of the deformation.

X. CONCLUSION

Based on the above results obtained from material model and experimental runs, it can be concluded that there is some degree of correlation between the two sets of the results. However correlation decreases when extreme variable settings are used for tool closing speed and tool temperature. This may be corrected by incorporating some degree of material cure into equation 2 to account for material viscosity and hence, shear stress induced by the material flow onto the embedded antenna.

Antenna deformation appears to have a very small impact on antenna signal quality and can be neglected when a wideband antenna is used but should be taken into consideration if a narrowband antenna is used in an end application.

ACKNOWLEDGMENT

The authors wish to thank Andrew Chryss for his technical support and guidance during rheological testing. This work is funded by the Australian Research Council, Grant Number LP0561868 and Composites Materials Engineering, CME.

REFERENCES

[1] Sarah, B., Lisa, M.A., Jose, M. C., Predicting molding forces during sheet molding compound (SMC) compression molding. II:effect of SMC composition, Polymer Composites, 24; 6; 2003 p.731-747
[2] Lindenmeier, H., Hopf, J., Reiter, L., Active AM-FM windshield antenna with equivalent performance to the whip now as standard equipment in car production, Antennas and Propagation Society International Symposium, 1985 p. 621- 624.
[3] Economou, L., Langley, J., Circular microstrip patch antennas on glass for vehicle applications, IEE Proceedings - Microwaves, Antennas and Propagation, 145; 5; 1998 p. 416-420.
[4] Walbeoff, A., Langley, R.J., Multiband PCB antenna, IEE Proceedings - Microwaves, Antennas and Propagation, 2005 p. 471- 475.
[5] Low, L., Langley, R., Breden, R., Callaghan, P., Hidden Automotive Antenna Performance and Simulation, IEEE Transaction on Antennas and Propagation, 54; 12; 2006 p. 3707-3712.
[6] Gschwendtner, E., Wiesbeck, W., "Ultra-broadband car antennas for communications and navigation applications," *IEEE Transaction on Antennas and Propagation*, Volume 51, Issue 8, August 2003, pp. 2020-2027.
[7] Barone, R., M, and Caulk, D.A., "The Effect of Deformation and Thermoset Cure on Heat Conduction in a Chopped-Fiber Reinforced Polyester during Compression Molding", *International Journal of Heat and Mass Transfer*, Volume 22, 1979, pp. 1021-1032.
[8] Barone, R., M, and Caulk, D.A.,"Kinematics of Flow in Sheet Molding Compound", *Polymer Composites*, Volume 6, 1985, pp. 105-109.
[9] Barone, R., M, and Caulk, D.A., "A Model for the Flow of a Chopped Reinforced Polymer Compound in Compression Molding", *Journal of Applied Mechanics,* Volume 53, 1986, p. 361
[10] Osswald, T. A., "Numerical Methods for Compression Mold Filling Simulation" Mechanical Engineering, 1987.
[11] Castro, J. M., and Griffith, R. M., "Sheet Molding Compound Compression-. Molding Flow", *Polymer Engineering and Science*, Volume 29, Issue 10, 1989.
[12] Castro, J. M., and Tomlinson, G., "Predicting molding forces during sheet molding compound (SMC) compression molding. I: Model development", *Polymer Engineering and Science,* Volume 30, Issue 24, 1990, pp. 1569-1573.
[13] Tucker, C. L., and Liang, E. W., " A Finite Element Method for Flow in Compression Molding of Thin and Thick Parts', *Polymer Composites,* Volume 16, 1995, pp.70-80.
[14] Bird, B, R., Armstrong, C, R., and Hassager, O., Dynamics of polymeric liquids, Wiley, 1987, p. 258-263
[15] Fundrinier, E., Venet, C., and Silva, L., "3D Computation of reactive moulding process", *Springer,* Volume 10, 2008, pp.735-738.